9-1-2002

Effect of grain growth inhibitors on the hysteresis properties of $Nd_{10}Fe_{82}C_6B_2$melt-spun alloys

M. Daniil
Department of Physics and Astronomy, University of Delaware, Newark, DE

Y. Zhang
Department of Physics and Astronomy, University of Delaware, Newark, DE

H. Okumura
Department of Physics, University of Delaware, Newark, DE

George C. Hadjipanayis
University of Delaware, hadji@udel.edu

David J. Sellmyer
University of Nebraska-Lincoln, dsellmyer@unl.edu

Effect of Grain Growth Inhibitors on the Hysteresis Properties of $Nd_{10}Fe_{82}C_6B_2$ Melt-Spun Alloys

M. Daniil, Y. Zhang, H. Okumura, G. C. Hadjipanayis, *Member, IEEE,* and D. J. Sellmyer, *Member, IEEE*

***Abstract*—An effort has been made to improve the coercivity of nanocomposite $Nd_{10}Fe_{82}C_6B_2$ alloys, using small amounts (up to 1 at%) of Cr, Ti, Nb, Zr, and Ga. X-ray studies revealed that the amount of α–Fe phase in both as-spun and annealed ribbons was significantly reduced for Nb and Zr substitutions, but increased for all the other substitutions. From the magnetic properties point of view, Zr (1 at%) was proven to be the most advantageous of all, since it increased the coercivity of annealed ribbons from 3.2 to 4.8 kOe and the maximum energy product from 5.8 to 13 MGOe. This improvement is associated with the much finer and more uniform microstructure as was revealed by transmission electron microscopy.**

***Index Terms*—2 : 14 : 1 carbides, grain growth inhibitors, nanocomposite magnets.**

I. Introduction

NANOCOMPOSITE magnets consisting of a fine mixture of a hard and a soft phase are very well known for their excellent magnetic properties; i.e., enhanced remanence, reasonably high coercivity in combination with low cost and corrosion resistance, because of the smaller amount of rare-earth. The remanence enhancement is related to the exchange coupling between the two constituent phases and it depends strongly on the grain size and distribution of the soft phase. Optimum magnetic properties have been obtained when the grains of the soft phase are less than 20 nm [1].

Nanocomposite magnets obtained with the melt-spinning technique have a rather nonuniform microstructure and the grain size of the soft phase is too large for optimum exchange coupling [2]. Recent studies have shown that small substitutions (up to 1 at%) with some elements (known as grain growth inhibitors), such as Nb [3]–[5], Zr [5], [6], Ti [1], [5] Ga [7], [8], and Cr [5], [9] for Fe can actually lead to a finer and more uniform microstructure with improved magnetic properties.

In our previous paper, the effect of carbon on the formation and magnetic properties of nanocomposite Nd_2Fe_{14} (C,B)/α–Fe magnets with composition $Nd_{10}Fe_{82}B_{8-y}C_y$ $(y = 0, 2, 4, 5, 6, 7)$ was examined [10]. The magnetic measurements showed that the coercivity had a maximum of 8.7 kOe for $y = 2$, followed by a gradual decrease with further increase of carbon concentration. The deterioration of the magnetic properties with y was found to be associated with the change of the crystallization behavior and the coarsening and nonuniformity of the microstructure for $y > 4$. Similar results were observed by Wang *et al.* in [11].

In this paper, we chose a composition with high carbon content (i.e., $Nd_{10}Fe_{82}B_2C_6$) and, therefore, with inferior magnetic properties, and we investigated the effect of small substitutions (i.e., Zr, Nb, Cr, Ga, and Ti) for iron, on the magnetic, structural, and microstructural properties of the ribbons.

II. Experiment

Master alloys with composition $Nd_{10}Fe_{82-x}M_xB_2C_6$, with M = Ga, Ti, Cr, Zr and Nb and $x = 0, 0.5, 1$, were prepared by arc-melting the elements Nd, Fe, and the dopants M with the alloys Fe–C and Fe–B, under argon pressure. The ingots were remelted four to five times and then solutionized at 1050 °C, under argon, for 24 h to ensure homogeneity. Small pieces (0.7–0.8 gr) of the arc-melted buttons were melt-spun into ribbons under argon atmosphere, using a single roller Cu wheel. A range of wheel-speeds, from 12 to 26 m/s, was used to optimize the magnetic properties. For the injection of the molten alloy, helium gas was used. The as-spun ribbons were sealed under vacuum and annealed at temperatures in the range of 750 °C–900 °C for 30 s–2 min and then cooled in air. The phases of the samples were identified by a Philips X-ray diffractometer (XRD) using Kα Cu radiation, whereas the verification of the existence of magnetic phases was done by thermomagnetic measurements. These measurements were carried out with a high-temperature vibrating sample magnetometer (VSM) under argon flow using an applied field of 0.8 kOe. The hysteresis loops were measured in small ribbon pieces with a VSM using maximum fields of 50 kOe. Their long axis was oriented parallel to the external field. The saturation magnetization, M_s was determined from M versus $1/H^2$ plots and extrapolation to infinite fields. Finally, microstructural studies were performed with a JEOL JEM-2000 FX transmission electron microscope (TEM).

III. Results and Discussion

The XRD patterns of as-spun ribbons with $x = 0$ and M = Nb, Zr with $x = 0.5$ and 1 showed a similar behavior with the wheel speed. At low speeds, there is a mixture of three phases, 2 : 14 : 1, 2 : 17 : C_x, and α–Fe. As the wheel speed increases, the 2 : 14 : 1 disappears. In Fig. 1(a) and (b) two representative

Manuscript received February 15, 2002; revised May 27, 2002. This work was supported by the U.S. Department of Energy under Grant DE-FG02-90ER4513.

M. Daniil, Y. Zhang, and G. C. Hadjipanayis are with the Department of Physics and Astronomy, University of Delaware, Newark, DE 19716 USA (e-mail: mdaniil@udel.edu; yzhang@physics.udel.edu; hadji@udel.edu).

H. Okumura was with the Department of Physics, University of Delaware, Newark, DE 19716 USA. He is now with the Department of Materials Science and Engineering, Carnegie Mellon University, Pittsburgh, PA 15213 USA (e-mail: okumura@ece.cmu.edu).

D. J. Sellmyer is with the Center of Materials Research and Analysis of Nebraska, University of Nebraska, Lincoln, NE 68588 USA (e-mail: dsellmyer1@unl.edu).

Digital Object Identifier 10.1109/TMAG.2002.803315.

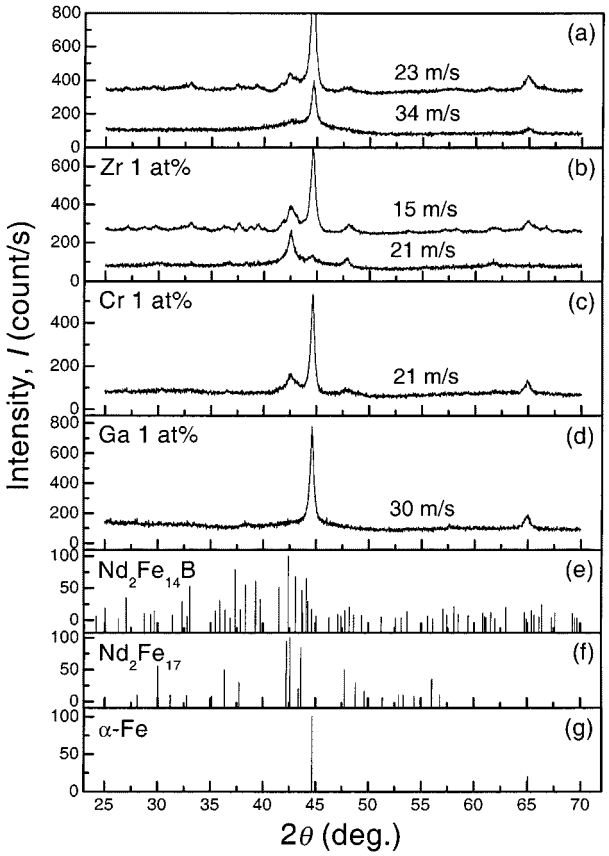

Fig. 1. XRD patterns of melt-spun (a) $Nd_{10}Fe_{82}B_2C_6$; (b) $Nd_{10}Fe_{81}ZrB_2C_6$; (c) $Nd_{10}Fe_{81}CrB_2C_6$; (d) $Nd_{10}Fe_{81}GaB_2C_6$ ribbons. The reference patterns of the $Nd_2Fe_{14}B$, Nd_2Fe_{17}, and α–Fe phases are shown in (e), (f), and (g), respectively.

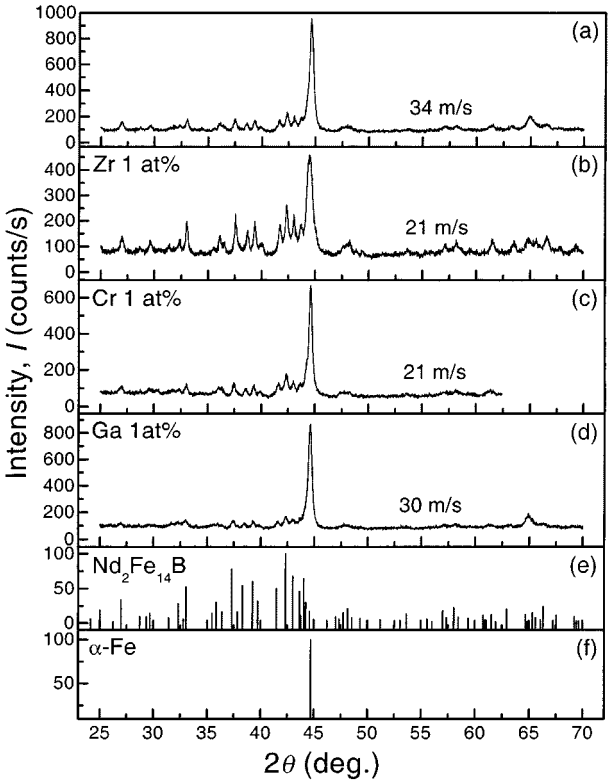

Fig. 2. XRD patterns of optimally melt-spun ribbons followed by optimal annealing: (a) $Nd_{10}Fe_{82}B_2C_6$; (b) $Nd_{10}Fe_{81}ZrB_2C_6$; (c) $Nd_{10}Fe_{81}CrB_2C_6$; (d) $Nd_{10}Fe_{81}GaB_2C_6$ ribbons. The reference patterns of the $Nd_2Fe_{14}B$, and α–Fe phases are shown in (e), and (f), respectively.

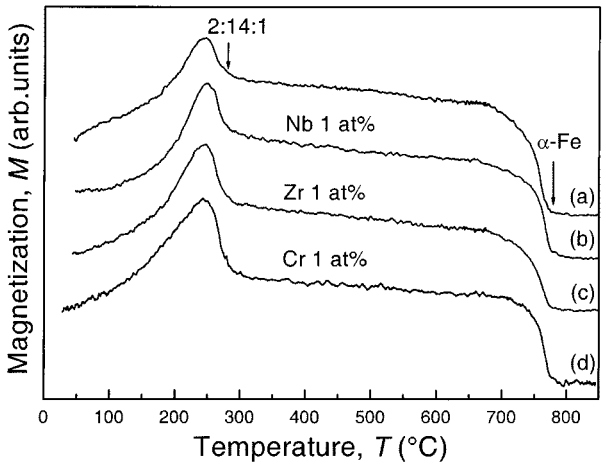

Fig. 3. Thermomagnetic curves of annealed $Nd_{10}Fe_{82}B_2C_6$ ribbons (a) without any substitutions; (b) with Nb; (c) Zr; and (d) Cr substitutions.

X-ray patterns are shown; one without any substitutions and one with 1 at% of Zr, melt-spun at two different wheel speeds. One significant difference between these two patterns is that the amount of α–Fe decreases drastically when Zr and Nb additions are used. On the contrary, when Ga, Cr, and Ti substitutions were used, there were no traces of the 2 : 14 : 1 phase, at any wheel speed. Instead, the 2 : 17 : C_x phase appeared together with larger amounts of α–Fe phase (the main phase). Typical patterns with Ga and Cr can be seen in Fig. 1(c) and (d).

After short time (1 min) annealing at 800 °C the soft 2 : 17 : C_x phase transforms into the hard 2 : 14 : 1. Fig. 2 shows the X-ray patterns of the annealed optimally quenched ribbons with and without substitutions. All the annealed ribbons are composed of the 2 : 14 : 1 phase and α–Fe. The amount of the latter phase increases for Ga and Cr additions, decreases for Nb and Zr, and remains almost the same with Ti.

The existence of the magnetic phases in the annealed ribbons was also verified by Curie temperature measurements in the M versus T experiments. Fig. 3 shows some M–T curves of annealed samples with 0 and 1 at% of substitutions. The M versus T data showed only two magnetic transitions present: one at ~280 °C, which corresponds to the 2 : 14 : 1 phase and another at 770 °C characteristic for the α–Fe. Consequently all the soft 2 : 17 : $C_x$transformed into the magnetically hard 2 : 14 : 1 phase. It can also be observed that the above substitutions do not change the Curie temperature of any of the phases. This is an indication that the dopant additions do not enter into the crystal structure of either the 2 : 14 : 1 or α–Fe phases.

Bright field micrographs of the Nb, Zr and Ti containing ribbons (after optimal annealing) are shown in Fig. 4(b) and (c), respectively, and are compared with the micrograph of the initial composition (without any substitutions) in Fig. 4(a). The ribbons without any additions ($Nd_{10}Fe_{82}B_2C_6$) did not show very uniform size distribution (60–100 nm) of 2 : 14 : 1 and α–Fe phase [Fig. 4(a)]. The average grain size is ~85 nm. When some Nb is added (0.5 at%) [Fig. 4(b)] the microstructure remains nonuniform but with rather smaller grains. The average grain

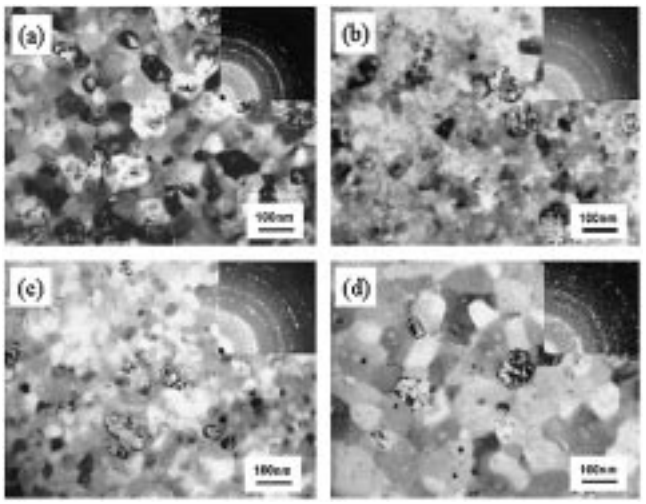

Fig. 4. Bright field images of optimally processed ribbons, with composition: (a) $Nd_{10}Fe_{82}B_2C_6$; (b) $Nd_{10}Fe_{81.5}Nb_{0.5}B_2C_6$; (c) $Nd_{10}Fe_{81}ZrB_2C_6$; and (d) $Nd_{10}Fe_{82}Ti_{0.5}B_2C_6$.

TABLE I
EFFECT OF SMALL SUBSTITUTIONS ON THE MAGNETIC PROPERTIES OF OPTIMALLY QUENCHED AND ANNEALED $Nd_{10}Fe_{82-x}M_xC_6B_2$ RIBBONS

mposition	M_s emu/g	M_r emu/g	m_r	H_c kOe	$(BH)_{max}$ MGOe
$Nd_{10}Fe_{82}C_6B_2$	150	76.5	0.51	3.2	4.3
$Nd_{10}Fe_{81.5}Zr_{0.5}C_6B_2$	154	90	0.58	4.1	6.9
$Nd_{10}Fe_{81}ZrC_6B_2$	164	101.6	0.62	4.8	13
$Nd_{10}Fe_{81.5}Nb_{0.5}C_6B_2$	156	88.8	0.57	4.1	8.7
$Nd_{10}Fe_{81}NbC_6B_2$	157	90	0.59	4.2	8.5
$Nd_{10}Fe_{81.5}Ti_{0.5}C_6B_2$	166	75.5	0.45	3.1	6.4
$Nd_{10}Fe_{81}CrC_6B_2$	159	72.5	0.45	2.2	4.0
$Nd_{10}Fe_{81}GaC_6B_2$	160	93	0.47	2.2	3.9

size of the 2 : 14 : 1 phase is 65 nm, but some huge α–Fe grains (>100 nm) are still present. In addition, some NbC precipitates were found, shown as small black dots. A more drastic change in the microstructure was observed for Zr substitutions (1 at%) [Fig. 4(c)]. The grains are finer and more uniform with an average size of 40 nm for the 2 : 14 : 1 grains and 88 nm for the α–Fe. No ZrC precipitates were found. On the contrary when Ti is added (0.5 at%) the microstructure gets coarser (average size ~110 nm for both 2 : 14 : 1 and α–Fe). In addition to the 2 : 14 : 1 and α–Fe grains, many TiC precipitates were found.

Table I summarizes the magnetic properties of the annealed ribbons that were optimally quenched, for different substitutions, whereas some representative magnetic hysteresis loops are presented in Fig. 5. The best properties for Nb, Zr, and Ti were obtained after annealing at 800 °C for 1 min, but for Ga and Cr additions annealing at higher temperatures (900 °C and 860 °C, respectively) was necessary.

The best magnetic properties were achieved for 1 at% of Zr substitution; the coercivity increased up to 4.8 kOe and the reduced remanence m_r up to 0.62 (dashed line in Fig. 5). These two facts in combination with the high saturation magnetization tripled the maximum energy product to 13 MGOe, as compared to 4.3 MGOe obtained without any substitutions. The enhanced

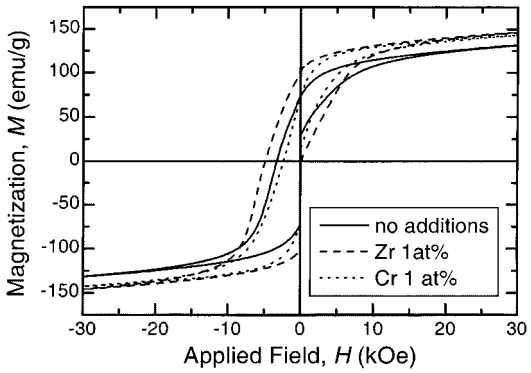

Fig. 5. Magnetic hysteresis loops of the optimally processed ribbons: (solid line) no substitutions; (dashed line) with 1 at% of Zr; and (dotted line) 1 at% of Cr substitutions.

m_r values for Nb and Zr containing samples indicate stronger exchange coupling between the 2 : 14 : 1 and α–Fe grains. The improved magnetic properties, for the Zr substitution is a consequence of the much finer and more uniform microstructure mentioned earlier. In contrast to Nb and Zr additions, Ti and especially Cr and Ga deteriorate all the magnetic parameters. This can be associated with the much coarser microstructure. The main reason for this behavior is the formation of M-carbides which use the amount of carbon needed for the formation of the 2 : 14 : 1 phase.

REFERENCES

[1] J. M. Yao, T. S. Chin, and S. K. Chen, "Coercivity of Ti-modified (α-Fe)-$Nd_2Fe_{14}B$ nanocrystalline alloys," *J. Appl. Phys.*, vol. 76, pp. 7071–7073, 1994.

[2] G. C. Hadjipanayis, "Nanophase hard magnets," *J. Magn. Magn. Mater.*, vol. 200, pp. 373–391, 1999.

[3] Z. M. Chen, Y. Zhang, Y. Q. Ding, G. C. Hadjipanayis, Q. Chen, and B. M. Ma, "Studies on the magnetic properties and microstructure of melt-spun nanocomposite $R_8(Fe, Co, Nb)_{86}B_6$ (R=Nd, Pr) magnets," *J. Magn. Magn. Mater.*, vol. 195, pp. 420–427, 1999.

[4] Z. M. Chen, Y. Zhang, G. C. Hadjipanayis, Q. Chen, and B. M. Ma, "Exchange coupled $R_2(Fe, Co, Nb)_{14}/(Fe, Co)$ (R=Nd, Pr) and $Sm_2(Fe, Co, Cr)_{17}C_2/(Fe, Co)$ nanocomposite magnets," *J. Alloys Comp.*, vol. 287, pp. 227–233, 2001.

[5] Z. M. Chen, H. Okumura, G. C. Hadjipanayis, and Q. Chen, "Microstructure refinement and magnetic property enhancement of nanocomposite $Pr_2Fe_{14}B/\alpha$-Fe magnets by small substitution of M for Fe (M=Cr, Nb, Ti and Zr)," *J. Alloys Comp.*, vol. 327, pp. 201–205, 2001.

[6] C. L. Harland and H. A. Davies, "Effect of Co and Zr on the magnetic properties of nanophase PrFeB alloys," *J. Appl. Phys.*, vol. 87, pp. 6116–6118, 2000.

[7] I. Panagiotopoulos, A. S. Murthy, and G. C. Hadjipanayis, "Magnetic properties and microstructure of melt-spun Nd–Fe–Ga–B alloys," *IEEE Trans. Magn.*, vol. 31, pp. 3617–3619, 1995.

[8] E. H. C. P. Sinnecker, E. Ferrara, R. Tiberto, M. Baricco, and F. Vinai, "Magnetic properties of Ga substituted Nd–Fe–B composite," *J. Magn. Magn. Mater.*, vol. 196-197, pp. 291–292, 1999.

[9] W. C. Chang, S. H. Wu, B. M. Ma, and C. O. Bounds, "Magnetic properties enhancement of nanocomposite $Nd_{9.5}Fe_{81.5}B_9$ melt-spun ribbons by LA and Cr substitutions," *J. Appl. Phys.*, vol. 81, pp. 4453–4455, 1997.

[10] M. Daniil, H. Okumura, G. C. Hadjipanayis, and D. J. Sellmyer, "Effect of carbon substitution on the magnetic properties of $Nd_2Fe_{14}(B, C)/\alpha$-Fe nanocomposite magnets," *J. Magn. Magn. Mater.*, submitted for publication.

[11] Z. C. Wang, H. A. Davies, and S. Z. Zhou, "Effect of C content on the formation and magnetic properties of $Nd_2Fe_{14}(BC)/\alpha$-Fe nanocomposite magnets," *J. Appl. Phys.*, vol. 91, pp. 3769–3774, 2002.